

Gravitational waves from (MHD) turbulence and magnetic fields in the early Universe

Hearing beyond the standard model with cosmic sources of Gravitational Waves

ICTS (January 9, 2025)



Alberto Roper Pol
University of Geneva



SNSF Ambizione grant (2023–2026): “*Exploring the early universe with gravitational waves and primordial magnetic fields.*”

Probing the early Universe with GWs

Cosmological (pre-recombination) GW background

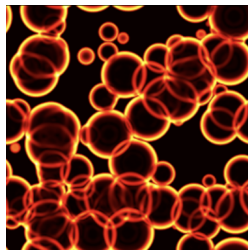
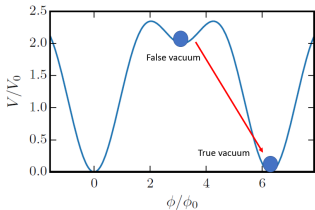
- Why background? Individual sources are not resolvable, superposition of single events occurring in the whole Universe.

$$f_* \simeq 1.64 \times 10^{-3} \frac{100}{R_* \mathcal{H}_*} \frac{T_*}{100 \text{ GeV}} \text{ Hz}$$

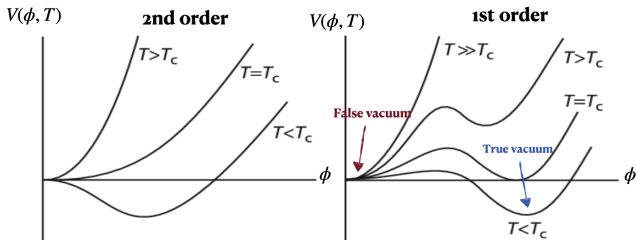
- Phase transitions
 - Ground-based detectors (LVK, ET, CE) frequencies are 10–1000 Hz
Peccei-Quinn, B-L, left-right symmetries $\sim 10^7, 10^8$ GeV.
 - Space-based detectors (**LISA**) frequencies are 10^{-5} – 10^{-2} Hz
Electroweak phase transition ~ 100 GeV
 - Pulsar Timing Array (**PTA**) frequencies are 10^{-9} – 10^{-7} Hz
Quark confinement (QCD) phase transition ~ 100 MeV

First-order phase transition [T. Konstandin's lectures]

$$V(\phi, T) = \frac{1}{2}M^2(T)\phi^2 - \frac{1}{3}\delta(T)\phi^3 + \frac{1}{4}\lambda\phi^4$$



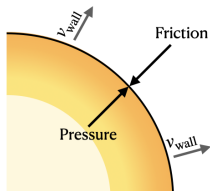
Credits: I. Stomberg



Hydrodynamics of first-order phase transitions¹

[T. Konstandin's lectures]

- Broken-phase bubbles are nucleated and expand
- Friction from particles yield a terminal velocity ξ_w of the bubbles
- The bubble can run away when the friction is not enough to stop the bubble's acceleration



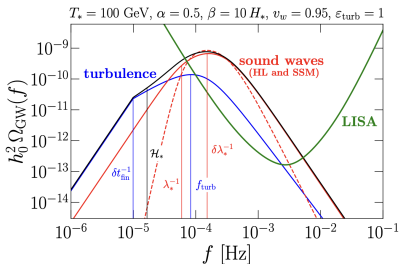
$$\nabla_{\mu} T_{\text{field}}^{\mu\nu} = \frac{\partial V}{\partial \phi} \partial^{\nu} \phi + \eta u^{\mu} \partial_{\mu} \phi \partial^{\nu} \phi,$$
$$\nabla_{\mu} T_{\text{fluid}}^{\mu\nu} = -\frac{\partial V}{\partial \phi} \partial^{\nu} \phi - \eta u^{\mu} \partial_{\mu} \phi \partial^{\nu} \phi,$$

¹Espinosa, Konstandin, No, Servant, *JCAP* 06 (2010) 028.

GW sources in the early Universe

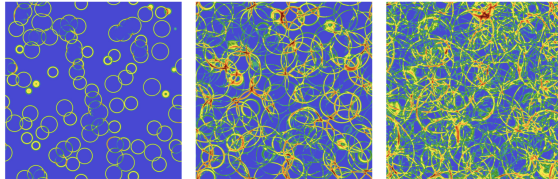
- Magnetohydrodynamic (MHD) sources of GWs:
 - Sound waves generated from first-order phase transitions.
 - (M)HD turbulence from first-order phase transitions.
 - Primordial magnetic fields.
- High-conductivity of the early universe leads to a high-coupling between magnetic and velocity fields.
- Other sources of GWs include
 - Bubble collisions.
 - Cosmic strings.
 - Primordial black holes.
 - Inflation.

ARP *et al.*, 2307.10744, 2308.12943

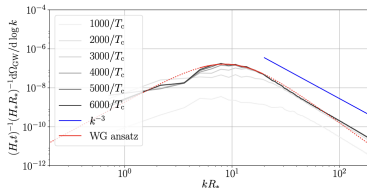


GWs from sound waves² [T. Konstandin's lectures]

- Numerical simulations of the scalar + fluid system performed by the Sussex/Helsinki group via an effective friction term.



- Two scales are found that determine the GW spectrum: R_* and ΔR_* (sound-shell thickness).



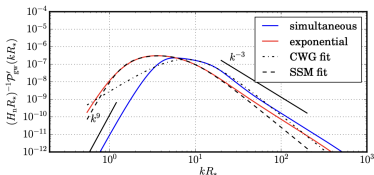
(b) Intermediate, $v_w = 0.92$

GWs from sound waves: Sound Shell Model³

- The sound shell model assumes linear superposition of velocity fields from each of the single bubbles and averages over nucleation locations and bubble lifetimes (semi-analytical model), and the development of sound waves at the time of collisions. It assumes stationary UETC $P_{\Pi} = P_{\Pi}(k, t_2 - t_1)$.

$$\Omega_{\text{GW}}(f) = 3 \tilde{\Omega}_{\text{GW}} K^2 (H_* \tau_{\text{sw}}) (H_* R_*) S(f R_*)$$

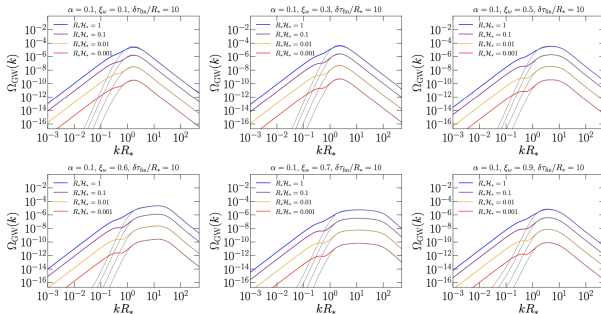
- It predicted a steep k^9 spectrum and linear growth with time, according to HH19, and k^{-3} at large frequencies, with an intermediate k between $1/R_*$ and $1/\Delta R_*$.
- GW predictions usually assume $\tau_{\text{sw}} = \min(\tau_{\text{sh}}, H_*^{-1})$, with $\tau_{\text{sh}} \sim R_*/\sqrt{K}$ being the expected time to develop non-linearities (should be a conformal time interval $\tau_{\text{sw}} = \tau_{\text{fin}} - \tau_*$ due to the conformal invariance of the fluid equations!).



(b) Intermediate, $v_w = 0.92$

GWs from sound waves: Sound Shell Model revisited⁴

- Extended Sound Shell model to an expanding Universe and omitted assumptions that were not holding at small k . Furthermore, an additional contribution to the GW spectrum is identified, omitted in previous studies.
- Recovered k^3 at small frequencies and found a $\ln^2(1 + \tau_{\text{SW}} H_*)$ time evolution of the causal branch and the “linear-in-time” evolution $\Upsilon = \tau_{\text{SW}} H_*/(1 + \tau_{\text{SW}} H_*)$ around the peak, as well as a sharp bump.



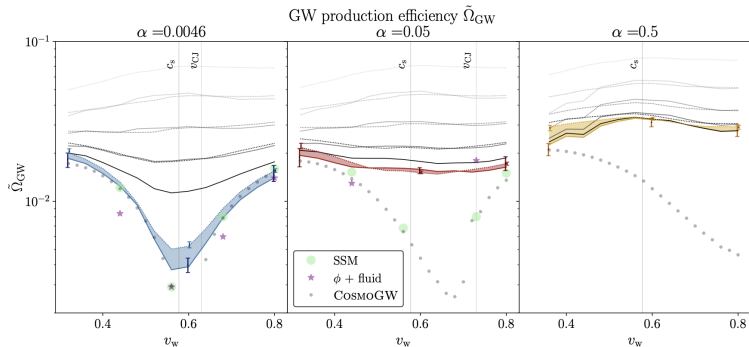
⁴ ARP, Procacci, Caprini, Phys. Rev. D, arXiv:2308.12943

Higgsless simulations (results)⁶

- In the literature, the GW spectrum from sound waves is usually assumed to be

$$\Omega_{\text{GW}}(f) = 3 \tilde{\Omega}_{\text{GW}} K^2 (H_* \tau_{\text{sw}}) (H_* R_*) S(f R_*)$$

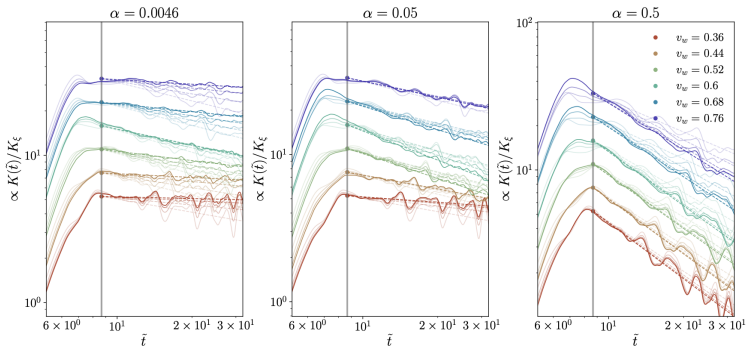
- $\tilde{\Omega}_{\text{GW}}$ is the efficiency factor



⁶ Caprini et al. (incl. ARP), arXiv:2409.03651 (2024).

Higgsless simulations (results)⁷

- Kinetic energy decay is observed in the simulations.
- For weak and strong PTs, increasing discretization enhances the decay.
- Potential indication of the development of non-linearities (turbulence).



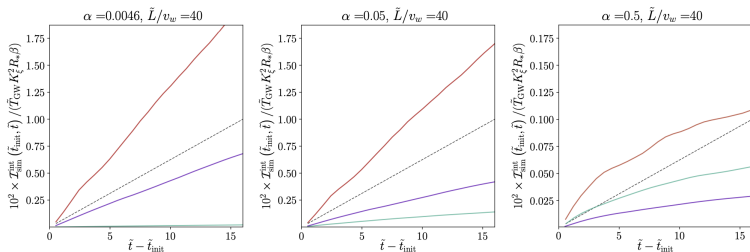
Higgsless simulations (results)⁸

- In the literature, the GW spectrum from sound waves is usually assumed to be

$$\Omega_{\text{GW}}(f) = 3 \tilde{\Omega}_{\text{GW}} K^2 (\mathbf{H}_* \tau_{\text{sw}}) (H_* R_*) S(f R_*)$$

- The linear growth, which only appears when expansion is neglected, is modified when the decay of the source is significant (e.g., due to the development of non-linearities).
- Extended \tilde{t} model to proposed locally stationary UETC


$$\Omega_{\text{GW}}(f) = 3 \tilde{\Omega}_{\text{GW}} \mathbf{K}_{\text{int}}^2 (H_* R_*) S(f R_*)$$



Primordial magnetic fields

- Magnetic fields can either be produced at or present during cosmological phase transitions.
- The magnetic fields are strongly coupled to the primordial plasma and effectively produce vortical motion, inevitably leading to the development of MHD turbulence.⁹
- Present magnetic fields can be amplified by primordial turbulence via dynamo.¹⁰

⁹ J. Ahonen and K. Enqvist, *Phys. Lett. B* **382**, 40 (1996).

¹⁰ A. Brandenburg *et al.* (incl. ARP), *Phys. Rev. Fluids* **4**, 024608 (2019); 

Generation of primordial magnetic fields

- Bubble collisions and velocity fields induced by first-order phase transitions can amplify seed magnetic fields.
- Parity-violating processes during the EWPT are predicted by SM extensions that account for baryogenesis and can produce helical magnetic fields through sphaleron decay or B+L anomalies.¹¹

$$\mathbf{B} = \nabla \times \mathbf{A} - i \frac{2 \sin \theta_w}{g v^2} \nabla \Phi^\dagger \times \nabla \Phi$$

- Axion fields can amplify and produce magnetic field helicity.¹²

$$\mathcal{L} \supset \frac{\phi}{f} F_{\mu\nu} \tilde{F}^{\mu\nu}$$

¹¹T. Vachaspati, *Phys. Rev. B* **265**, 258 (1991), T. Vachaspati, *Phys. Rev. Lett.* **87**, 251302 (2001), J. M. Cornwall, *Phys. Rev. D* **56**, 6146 (1997).

¹²M. M. Forbes and A. R. Zhitnitsky, *Phys. Rev. Lett.* **85**, 5268 (2000).

Generation of primordial magnetic fields

- Inhomogeneities in the Higgs field in low-scale electroweak hybrid inflation.¹³
- Magnetic fields from inflation can be present during phase transitions (non-helical¹⁴ and helical¹⁵).
- Chiral magnetic effect.¹⁶

¹³ M. Joyce and M. E. Shaposhnikov, *Phys. Rev. Lett.* **79**, 1193 (1997),
J. García-Bellido et al., *Phys. Rev. D* **60**, 123504 (1999).

¹⁴ M. S. Turner and L. M. Widrow, *Phys. Rev. D* **37**, 2743 (1988).

¹⁵ M. Giovannini, *Phys. Rev. D* **58**, 124027 (1998).

¹⁶ M. Joyce and M. E. Shaposhnikov, *PRL* **79**, 1193 (1997).

GWs from (M)HD turbulence

- Direct numerical simulations using the `PENCIL CODE`¹⁷ to solve:
 - ① Relativistic MHD equations adapted for radiation-dominated era (after electroweak symmetry is broken).
 - ② Gravitational waves equation.
- In general, large-scale simulations are necessary to solve the MHD nonlinearities (e.g., unequal-time correlators UETC and non-Gaussianities, which require simplifying assumptions in analytical studies).
- Currently, *CosmoLattice*-MHD module is under-development (work with D. Figueroa, K. Marschall, A. Midiri).

¹⁷Pencil Code Collaboration, *JOSS* **6**, 2807 (2020),
<https://github.com/pencil-code/>

MHD description

Right after the electroweak phase transition we can model the plasma using continuum MHD.

- Charge-neutral, electrically conducting fluid.
- Relativistic magnetohydrodynamic (MHD) equations.
- Radiation-dominated fluid

$$p = \rho c^2/3,$$

i.e., $c_s^2 = 1/3$ (ultrarelativistic EoS).

- Friedmann–Lemaître–Robertson–Walker metric

$$g_{\mu\nu} = \text{diag}\{-1, a^2, a^2, a^2\}$$

Contributions to the stress-energy tensor

$$T^{\mu\nu} = (\rho/c^2 + \rho) U^\mu U^\nu + p g^{\mu\nu} + \pi^{\mu\nu} + F^{\mu\gamma} F^\nu{}_\gamma - \frac{1}{4} g^{\mu\nu} F_{\lambda\gamma} F^{\lambda\gamma}$$

- From fluid motions:

$$T_{ij} = (\rho/c^2 + \rho) \gamma^2 u_i u_j + p \delta_{ij}$$

- Ultrarelativistic EoS:

$$p = \rho c^2 / 3$$

- Viscous stresses: $\pi_{ij} =$

$$\nu(\rho/c^2 + \rho)(u_{i,j} + u_{j,i})$$

- 4-velocity $U^\mu = \gamma(c, u^i)$
- 4-potential $A^\mu = (\phi/c, A^i)$

- From magnetic fields:

$$T_{ij} = -B_i B_j + \delta_{ij} B^2 / 2$$

- 4-current $J^\mu = (c\rho_e, J^i)$

- Faraday tensor

$$F_{\mu\nu} = \partial_\mu A_\nu - \partial_\nu A_\mu$$

Conservation laws for MHD turbulence

$$T^{\mu\nu}{}_{;\nu} = 0, \quad F^{\mu\nu}{}_{;\nu} = -J^\mu, \quad \tilde{F}^{\mu\nu}{}_{;\nu} = 0$$

In the limit of subrelativistic bulk flow:

$$\gamma^2 \sim 1 + (v/c)^2 + \mathcal{O}(v/c)^4$$

Relativistic MHD equations are reduced to¹⁸

$$\begin{aligned} \frac{\partial \ln \rho}{\partial t} &= -\frac{4}{3} (\nabla \cdot \mathbf{u} + \mathbf{u} \cdot \nabla \ln \rho) + \frac{1}{\rho} [\mathbf{u} \cdot (\mathbf{J} \times \mathbf{B}) + \eta \mathbf{J}^2], \\ \frac{D\mathbf{u}}{Dt} &= \frac{\mathbf{u}}{3} (\nabla \cdot \mathbf{u} + \mathbf{u} \cdot \nabla \ln \rho) - \frac{\mathbf{u}}{\rho} [\mathbf{u} \cdot (\mathbf{J} \times \mathbf{B}) + \eta \mathbf{J}^2] \\ &\quad - \frac{1}{4} \nabla \ln \rho + \frac{3}{4\rho} \mathbf{J} \times \mathbf{B} + \frac{2}{\rho} \nabla \cdot (\rho \nu \mathbf{S}), \\ \frac{\partial \mathbf{B}}{\partial t} &= \nabla \times (\mathbf{u} \times \mathbf{B} - \eta \mathbf{J}), \quad \mathbf{J} = \nabla \times \mathbf{B}, \end{aligned} \tag{1}$$

for a flat expanding universe with comoving and normalized

$\rho = a^4 \rho_{\text{phys}}$, $\rho = a^4 \rho_{\text{phys}}$, $B_i = a^2 B_{i,\text{phys}}$, u_i , and conformal time t ($dt = a dt_c$).

¹⁸ A. Brandenburg, *et al.*, *Phys. Rev. D* **54**, 1291 (1996).

ARP, Midiri, in preparation, based on EPFL course

"Relativistic Magnetohydrodynamics in the early Universe." (2025).

3.2.1 Conformal invariance and conservation laws

An important aspect of the conservation laws of perfect fluids is that they are conformally invariant when the trace of the stress-energy tensor vanishes [10, 11]. To show this result, let us consider two metrics that are related by a conformal transformation as $g^{\mu\nu} = \Omega^2(x^\mu) \tilde{g}^{\mu\nu}$. This corresponds, for example, to the FLRW metric tensor $g^{\mu\nu}$ when we express the time coordinate as conformal time, where $\tilde{g}^{\mu\nu} = \eta^{\mu\nu}$ would correspond to flat Minkowskian space-time and $\Omega = a^{-1}(\tau)$ is the inverse scale factor. The conservation laws for a symmetric $T^{\mu\nu}$ given in a metric tensor $g^{\mu\nu}$ are

$$\begin{aligned} D_\mu T^{\mu\nu} &= \frac{1}{\sqrt{-g}} \partial_\mu (\sqrt{-g} T^{\mu\nu}) + \Gamma^\nu_{\mu\sigma} T^{\mu\sigma} \\ &= \frac{\Omega^4}{\sqrt{-\tilde{g}}} \partial_\mu (\sqrt{-\tilde{g}} \Omega^{-4} T^{\mu\nu}) + \tilde{\Gamma}^\nu_{\mu\sigma} T^{\mu\sigma} - 2 T^{\mu\nu} \partial_\mu \ln \Omega + T^\mu_{\mu} \partial^\nu \ln \Omega, \end{aligned} \quad (3.16)$$

where $\tilde{\Gamma}^\nu_{\mu\sigma}$ are the Christoffel symbols of the metric tensor $\tilde{g}^{\mu\nu}$. Introducing the comoving stress-energy tensor $\tilde{T}^{\mu\nu} = \Omega^{-6} T^{\mu\nu}$, we find

$$D_\nu T^{\mu\nu} = 0 \Leftrightarrow D_{\tilde{\nu}} \tilde{T}^{\mu\nu} + \Omega^{-2} \tilde{T}^\nu_{\nu} \partial^\mu \ln \Omega = 0, \quad (3.17)$$

$$\tilde{T} = 3\tilde{p} - \tilde{\rho}$$

GW equation for a flat expanding Universe

- Assumptions: isotropic and homogeneous Universe.
- Friedmann–Lemaître–Robertson–Walker (FLRW) metric $\gamma_{ij} = a^2 \delta_{ij}$.
- Tensor-mode perturbations above the FLRW model:

$$g_{ij} = a^2 \left(\delta_{ij} + h_{ij}^{\text{phys}} \right), \quad |h_{ij}^{\text{phys}}| \ll |g_{ij}|$$

- GW equation is¹⁹

$$\left(\partial_t^2 - \frac{a''}{a} - c^2 \nabla^2 \right) h_{ij} = \frac{16\pi G}{a c^2} T_{ij}^{\text{TT}}$$

- h_{ij} are rescaled $h_{ij} = a h_{ij}^{\text{phys}}$.
- Comoving spatial coordinates $\nabla = a \nabla^{\text{phys}}$.
- Conformal time $dt = a dt_c$.
- Comoving stress-energy tensor components $T_{ij} = a^4 T_{ij}^{\text{phys}}$.
- Radiation-dominated epoch such that $a'' = 0$.

¹⁹L. P. Grishchuk, *Sov. Phys. JETP* **40**, 409 (1974).
ARP et al., *Geophys. Astrophys. Fluid Dyn.* **114**, 130 (2020).

Numerical results for decaying MHD turbulence²⁰

Initial conditions

- Initial stochastic magnetic (or velocity) field with fractional helicity σ_M .

$$kB_i(\mathbf{k}) = \left(\delta_{ij} - \hat{k}_i \hat{k}_j - i\sigma_M \varepsilon_{ijl} \hat{k}_l \right) g_j \sqrt{2\Omega_M(k)/k}$$

- Batchelor spectrum for magnetic (or vortical velocity) fields, i.e., $\Omega_M \propto k^5$ for small $k < k_* \sim \mathcal{O}(\xi_M^{-1})$.
- Kolmogorov spectrum in the inertial range, i.e., $\Omega_M \propto k^{-2/3}$.

²⁰ A. Brandenburg *et al.* (incl. ARP), *Phys. Rev. D* **96**, 123528 (2017).
ARP *et al.*, *Phys. Rev. D* **102**, 083512 (2020).
ARP *et al.*, *JCAP* **04** (2022), 019.
ARP *et al.*, *Phys. Rev. D* **105**, 123502 (2022).

Numerical results for decaying MHD turbulence

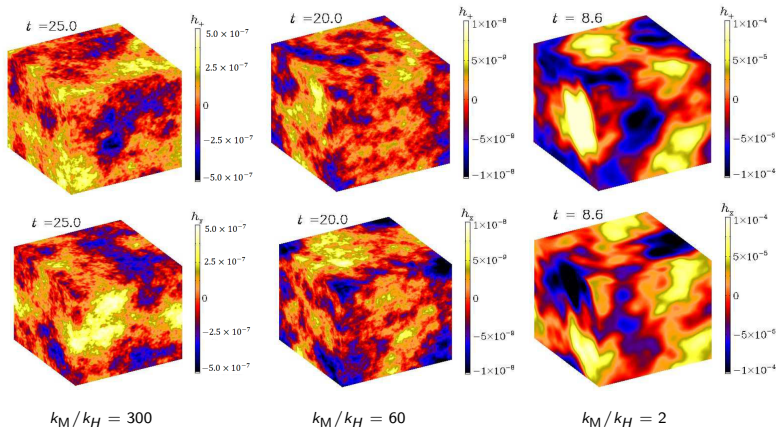
Free parameters on the initial conditions

- Magnetic energy density at t_* is a fraction of the radiation energy density, $\Omega_M = \mathcal{E}_M / \mathcal{E}_{\text{rad}}^* = \frac{1}{2} B_0^2 \leq 0.1$ (BBN limit).
- Fractional helicity of the initial magnetic field via σ_M .
- Spectral peak k_* , normalized by H_*/c , is given by the characteristic scale of the sourcing turbulence (as a fraction of the Hubble radius) and should be $k_* \geq 2\pi$ by causality.
- Time t_* at which the magnetic field is generated, corresponding to the temperature scale T_* (e.g., $T_* \sim 100$ GeV at the electroweak phase transition).

Numerical results for decaying MHD turbulence²¹

$$1152^3, \Omega_M \sim 10^{-2}, \sigma_M = 1$$

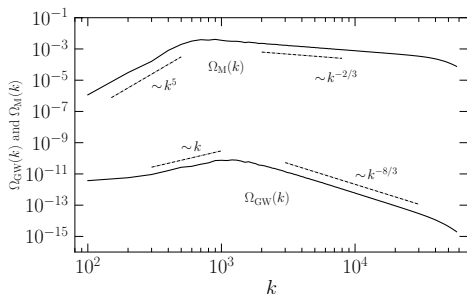
Box results for positive initial helicity:



²¹ ARP et al., *Phys. Rev. D* **102**, 083512 (2020).

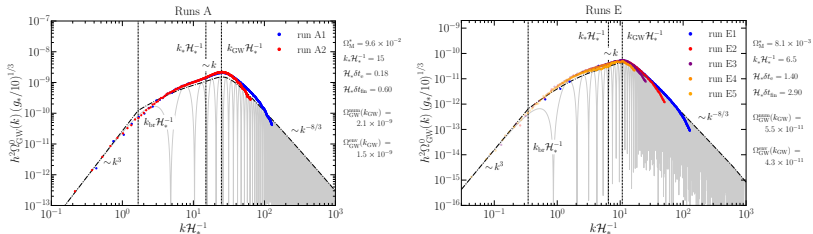
Numerical results for decaying MHD turbulence²²

$$1152^3, k_* = 2\pi \times 100, \Omega_M \sim 10^{-2}, \sigma_M = 1$$



- **Characteristic k scaling in the subinertial range for the GW spectrum.**
- k^2 expected at scales $k < k_*$ and k^3 at $k < H_*$ according to the “top-hat” model (Caprini *et al.*, 2020).

Numerical results for nonhelical decaying MHD turbulence²³



run	Ω_M^*	$k_* \mathcal{H}_*^{-1}$	$\mathcal{H}_* \delta t_e$	$\mathcal{H}_* \delta t_{fin}$	$\Omega_{GW}^{2D}(k_{GW})$	$[\Omega_{GW}^{2D}/\Omega_{GW}^{2D}](k_{GW})$	n	$\mathcal{H}_* L$	$\mathcal{H}_* t_{end}$	$\mathcal{H}_* \eta$
A1	9.6×10^{-2}	15	0.176	0.60	2.1×10^{-9}	1.357	768	6π	9	10^{-7}
A2	-	-	-	-	-	-	768	12π	9	10^{-6}
E1	8.1×10^{-3}	6.5	1.398	2.90	5.5×10^{-11}	1.184	512	4π	8	10^{-7}
E2	-	-	-	-	-	-	512	10π	18	10^{-7}
E3	-	-	-	-	-	-	512	20π	61	10^{-7}
E4	-	-	-	-	-	-	512	30π	114	10^{-7}
E5	-	-	-	-	-	-	512	60π	234	10^{-7}

Analytical model for GWs from decaying turbulence

- Assumption: magnetic or velocity field evolution $\delta t_e \sim 1/(u_* k_*)$ is slow compared to the GW dynamics ($\delta t_{\text{GW}} \sim 1/k$) at all $k \gtrsim u_* k_*$.
- We can derive an analytical expression for nonhelical fields of the envelope of the oscillations²⁴ of $\Omega_{\text{GW}}(k)$.

$$\Omega_{\text{GW}}(k, t_{\text{fin}}) \approx 3 \left(\frac{k}{k_*} \right)^3 \Omega_{\text{M}}^*{}^2 \frac{\mathcal{C}(\alpha)}{\mathcal{A}^2(\alpha)} p_{\Pi} \left(\frac{k}{k_*} \right) \\ \times \begin{cases} \ln^2[1 + \mathcal{H}_* \delta t_{\text{fin}}] & \text{if } k \delta t_{\text{fin}} < 1, \\ \ln^2[1 + (k/\mathcal{H}_*)^{-1}] & \text{if } k \delta t_{\text{fin}} \geq 1. \end{cases}$$

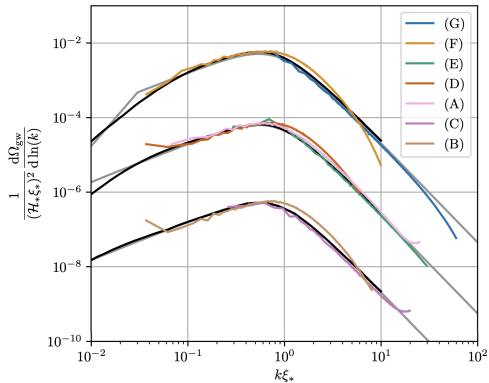
- p_{Π} is the anisotropic stress spectrum and depends on spectral shape, can be approximated for a von Kármán spectrum as²⁵

$$p_{\Pi}(k/k_*) \simeq \left[1 + \left(\frac{k}{2.2k_*} \right)^{2.15} \right]^{-11/(3 \times 2.15)}$$

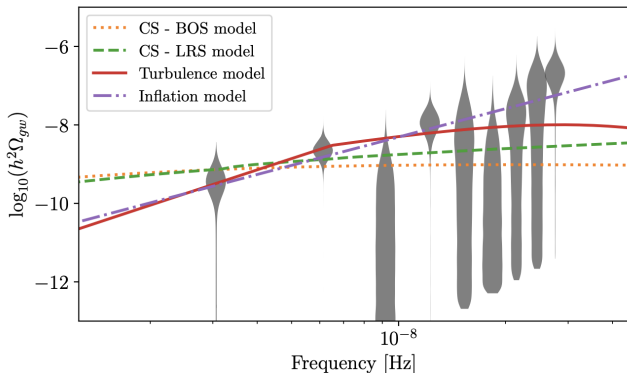
²⁴ ARP et al., *Phys. Rev. D* **105**, 123502 (2022).

²⁵ ARP et al., arXiv:2307.10744 (2023).

Numerical results for decaying HD vortical turbulence²⁶

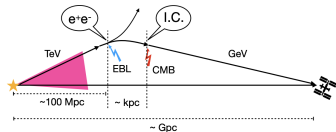


EPTA 24.7 yr data observation (DR 2)²⁸

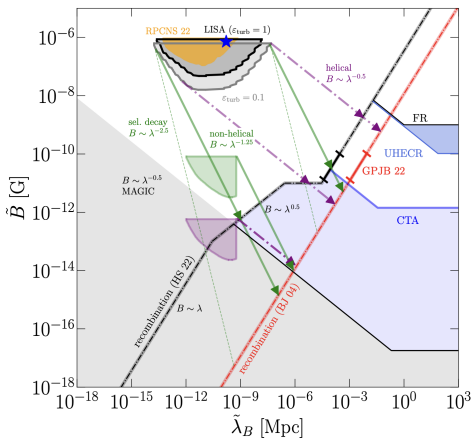


Primordial magnetic fields³⁰

- Primordial magnetic fields would evolve through the history of the universe up to the present time and could explain the lower bounds in cosmic voids derived by the Fermi collaboration.³¹



- Maximum amplitude of primordial magnetic fields is constrained by the big bang nucleosynthesis.³²
- Additional constraints from CMB, Faraday Rotation, ultra-high energy cosmic rays (UHECR).

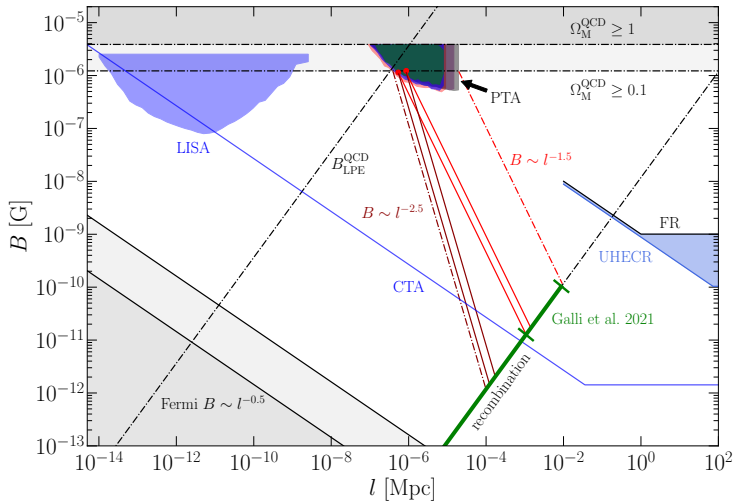


³⁰ ARP *et al.*, arXiv:2307.10744 (2023).

³¹ A. Neronov and I. Vovk, *Science* **328**, 73 (2010).

³² V. F. Shvartsman, *Pisma Zh. Eksp. Teor. Fiz.* **9**, 315 (1969).

Primordial magnetic field constraints with PTA²⁹



Conclusions

- Velocity and magnetic fields in the early universe can significantly contribute to the stochastic GW background (SGWB) via sound waves and (M)HD turbulence.
- The SGWB produced by turbulence requires, in general, performing high-resolution numerical simulations, which can be done using the `PENCIL CODE`.
- Since the SGWB is a superposition of different sources, it is extremely important to characterize the different sources, to be able to extract clean information from the early universe physics.
- The interplay between sound waves (acoustic motion) and the development of turbulence is not well understood. It plays an important role on the relative amplitude of both sources of GWs. On-going studies of phase transitions with `PENCIL CODE` are required to understand this issue.
- LISA, PTA, and next-generation ground-based detectors can be used to probe the origin of magnetic fields in the largest scales of our Universe, which is still an open question in cosmology.
- γ -ray observations (Fermi LAT, CTA) can constrain intergalactic magnetic fields, providing a potential multi-messenger approach to study primordial magnetic fields.



ಧನ್ಯವಾದಗಳು

alberto.roperpol@unige.ch

github.com/AlbertoRoper/cosmoGW
cosmology.unige.ch/users/alberto-roper-pol





Numerical simulations of early Universe sources of gravitational waves

July 28, 2025 to August 15, 2025 — Albano Building 3



[Main Page](#)

[Campus map](#)

[Practical Information](#)

[What is Nordita?](#)

[Directions to Nordita](#)

[Directions to BizApartment Hotel](#)

[Nordita Contact Information](#)

[Tourist Tips](#)

[Stockholm Tourist Info](#)

[Stockholm Public Transport](#)

Organized with [C. Caprini](#), [A. Drew](#), [D. Figueroa](#), [D. Weir](#)

Venue

Nordita, Stockholm, Sweden

SAVE THE DATE! JUL 28 - AUG 15, 2025

Scope

The main objectives of the program are:

- to study the different possible sources contributing to the cosmological GW background,
- to review the state-of-the-art numerical codes and techniques in the literature.

For this purpose, the program is divided into four weeks, covering the following potential sources of GWs in the early Universe:

1. Inflation and (p)reheating
2. Scalar perturbations and primordial black holes
3. First order phase transitions and primordial turbulence
4. Topological defects: cosmic strings and domain walls



The Pencil Code

a high-order finite-difference code for compressible MHD



Home

News

Documentation

Highlights

Samples

Autotests

Download

Meetings

References

Contact

Latest changes ...

Meetings



- 23-27 Sep, 2024: [20th meeting](#) [\[agenda\]](#) in Barcelona, Institute of Space Sciences (ICE-CSIC / IEEC) (Spain).
4-8 Sep, 2023: [19th meeting](#) [\[agenda\]](#) in Graz, Institute of Physics, University of Graz (Austria).
4-10 May, 2022: [18th meeting](#) [\[agenda\]](#) in Bangalore, IIA (India).
17-21 May, 2021: [17th meeting](#) [\[agenda\]](#) in Lausanne, EPFL (Switzerland).
27-31 Jul, 2020: [16th meeting](#) [\[agenda\]](#) in Glasgow, Glasgow University (UK).
12-16 Aug, 2019: [15th meeting](#) [\[agenda\]](#) in Espoo, Aalto University (Finland).
11-15 Jun, 2018: [14th meeting](#) [\[agenda\]](#) in Boulder, University of Colorado (USA).
10-14 Jul, 2017: [13th meeting](#) [\[agenda\]](#) in Newcastle, Newcastle University (UK).
08-12 Aug, 2016: [12th meeting](#) [\[agenda\]](#) in Graz, Space Research Institute, Academy of Sciences (Austria).
11-15 May, 2015: [11th meeting](#) [\[agenda\]](#) in Trondheim, Norwegian University of Science and Technology (Norway).
07-11 Jul, 2014: [10th meeting](#) [\[agenda\]](#) in Göttingen, Max Planck Institute for Solar System Research (Germany).
17-20 Jun, 2013: [9th meeting](#) [\[agenda\]](#) in Lund, Lund Observatory (Sweden).

<http://pencil-code.nordita.org/>

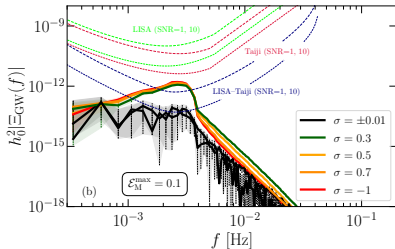
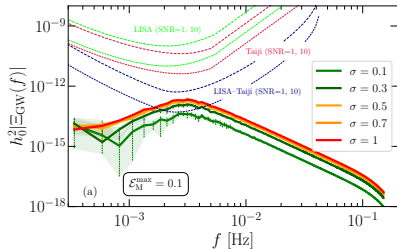
Next Pencil Code user meeting in Geneva,
Switzerland (2025), stay tuned!

Extra slides

Using LISA and Taiji to detect the GW polarization³²

- LISA's dipole response function can provide us with a polarized gravitational wave background due to our proper motion.³⁰
- Cross-correlation of LISA and an additional space-based GW detector can improve the detectability of a polarized GW background.³¹

$$\mathcal{P}_{\text{GW}}(k) = \frac{\Xi_{\text{GW}}(k)}{\Omega_{\text{GW}}(k)} = \frac{\langle \dot{\tilde{h}}_+^2 - \dot{\tilde{h}}_-^2 \rangle}{\langle \dot{\tilde{h}}_+^2 + \dot{\tilde{h}}_-^2 \rangle}$$



³⁰V. Domcke *et al.*, *JCAP* **05** (2020), 028.

³¹G. Orlando, M. Pieroni and A. Ricciardone, *JCAP* **03** (2021), 069.

³²ARP *et al.*, *JCAP* **04** (2022), 019.

Numerical results for forced MHD turbulence³³

Driven magnetic (or velocity) field

- Initial magnetic and velocity fields are zero.
- The magnetic field is forced during a short duration (e.g., $0.1H_*^{-1}$) via the induction equation:

$$\frac{\partial \mathbf{B}}{\partial t} = \nabla \times (\mathbf{u} \times \mathbf{B} - \eta \mathbf{J} + \mathcal{F}).$$

- The forcing term is quasi-monochromatic with fractional magnetic helicity σ .

$$\mathcal{F} = \text{Re}(\mathcal{A}\mathbf{f}) \exp[i\mathbf{k} \cdot \mathbf{x} + i\phi], \quad k_* - \frac{1}{2}\delta k \leq |\mathbf{k}| \leq k_* + \frac{1}{2}\delta k,$$

$$f_i = \left(\delta_{ij} - i\sigma \varepsilon_{ijl} \hat{k}_l \right) f_j^{(0)} / \sqrt{1 + \sigma^2}.$$

³³ ARP *et al.*, *Phys. Rev. D* **102**, 083512 (2020).

ARP *et al.*, *JCAP* **04** (2022), 019.

Forcing terms

Acoustic forcing³⁴ on velocity fields:

- Forcing from Gaussian potential

$$\mathbf{f} = \nabla\phi$$

$$\phi = N \exp([\mathbf{x} - \mathbf{x}_f]^2/R^2)$$

$$N = k_K/(2\pi)$$

- Monochromatic forcing in momentum equation.

$$\nabla \times \mathbf{u} = 0$$

Helical forcing³⁵ on magnetic fields:

- Fully helical forcing term (in Fourier space)

$$\mathbf{f}_k = \frac{\mathbf{k} \times (\mathbf{k} \times \hat{\mathbf{e}}) - ik(\mathbf{k} \times \hat{\mathbf{e}})}{2k^2 \sqrt{1 - (\mathbf{k} \cdot \hat{\mathbf{e}})^2/k^2}}$$

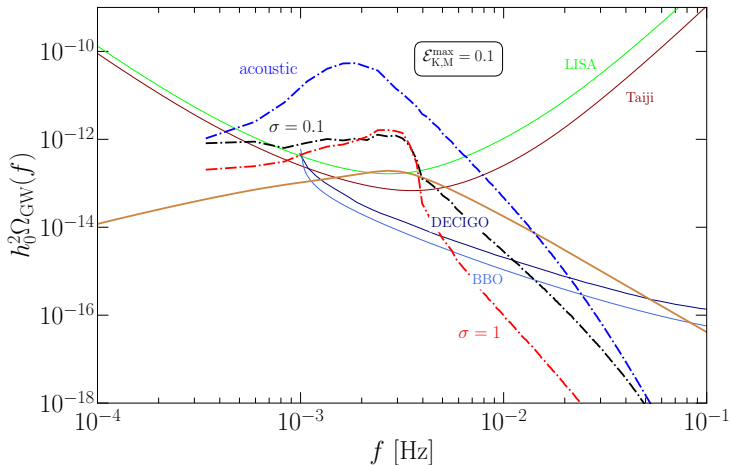
- Monochromatic forcing in induction equation.

$$\nabla \cdot \mathbf{B} = 0$$

³²A. J. Mee, A. Brandenburg, *Mon. Not. Roy. Astron. Soc.* **370**, 415 (2006).

³⁵A. Brandenburg, *Astrophys. J.* **550**, 824 (2001).

Using LISA to detect primordial magnetic fields at the
EWPT scale (forcing MHD turbulence)³⁶



³⁶ ARP *et al.*, *Phys. Rev. D* **102**, 083512 (2020).
 ARP *et al.*, *JCAP* **04** (2022), 019.
 ARP *et al.*, *Phys. Rev. D* **105**, 123502 (2022).